This Accepted Manuscript has not been copyedited and formatted. The final version may differ from this version.

eNeuro

Research Article: New Research | Sensory and Motor Systems

Optogenetic silencing of Nav1.8-positive afferents alleviates inflammatory and neuropathic pain

Light-induced analgesia in transgenic mice

Ihab Daou[1,2], Hélène Beaudry[1,2,3], Ariel R. Ase[1,2], Jeffrey S. Wieskopf[2,4], Alfredo Ribeiro-da-Silva[2,3], Jeffrey S. Mogil[2,4] and Philippe Séguéla[1,2]

[1]*Department of Neurology and Neurosurgery, Montreal Neurological Institute, H3A 2B4*
[2]*The Alan Edwards Centre for Research on Pain, H3A 0G1*
[3]*Department of Pharmacology and Therapeutics, H3G 1Y6*
[4]*Department of Psychology, H3A 1B1, McGill University, Montreal, Canada*

DOI: 10.1523/ENEURO.0140-15.2016

Received: 18 November 2015

Revised: 3 February 2016

Accepted: 19 February 2016

Published: 26 February 2016

Author contributions: I.D. and P.S. designed research; I.D., H.B., A.A., and J.W. performed research; I.D., H.B., A.A., J.W., A.R.-dS., J.S.M., and P.S. analyzed data; I.D. and P.S. wrote the paper; A.R.-dS. and J.S.M. contributed unpublished reagents/analytic tools.

Funding: CIHR: MOP-130239. Natural Sciences and Engineering Research Council of Canada: DG-203061. Fonds de Recherche du Quebec - Sante; (Fonds de la recherche en sante du Quebec): 501100000156. Arthritis Society of Canada; Quebec Pain Research Network; Louise and Alan Edwards Foundation;

Conflict of Interest: The authors declare no competing financial interests.

Corresponding author: Philippe Séguéla, Montreal Neurological Institute, 3801 University, Suite 778, Montreal, Quebec, Canada H3A 2B4. Tel 514 398 5029. Email: philippe.seguela@mcgill.ca

Cite as: eNeuro 2016; 10.1523/ENEURO.0140-15.2016

Alerts: Sign up at eneuro.org/alerts to receive customized email alerts when the fully formatted version of this article is published.

Accepted manuscripts are peer-reviewed but have not been through the copyediting, formatting, or proofreading process.

This is an open-access article distributed under the terms of the Creative Commons Attribution 4.0 International (http://creativecommons.org/licenses/by/4.0), which permits unrestricted use, distribution and reproduction in any medium provided that the original work is properly attributed.

Copyright © 2016 Society for Neuroscience

eNeuro Accepted Manuscript

eNeuro Accepted Manuscript

eNeuro

http://eneuro.msubmit.net

eN-NWR-0140-15R1

Optogenetic silencing of Nav1.8-positive afferents alleviates inflammatory and neuropathic pain

This is a confidential document and must not be discussed with others, forwarded in any form, or posted on websites without the express written consent of eNeuro.

eNeuro Accepted Manuscript

Optogenetic silencing of $Na_v1.8$-positive afferents alleviates inflammatory and neuropathic pain

Short title: **Light-induced analgesia in transgenic mice**

Ihab Daou,[1,2] Hélène Beaudry,[1,2,3] Ariel R. Ase,[1,2] Jeffrey S. Wieskopf,[2,4] Alfredo Ribeiro-da-Silva,[2,3] Jeffrey S. Mogil,[2,4] and Philippe Séguéla[1,2]

[1]Montreal Neurological Institute, Department of Neurology and Neurosurgery, H3A 2B4; [2]The Alan Edwards Centre for Research on Pain, H3A 0G1; [3]Department of Pharmacology and Therapeutics, H3G 1Y6; [4]Department of Psychology, H3A 1B1, McGill University, Montreal, Canada

Author contributions: I.D., H.B. and P.S. designed research; I.D., H.B., A.R.A. and J.S.W. performed research; I.D., H.B., A.R.A., A.R.-d.S., J.S.M. and P.S analyzed data; I.D. and P.S. wrote the paper.

Corresponding author: Philippe Séguéla
Montreal Neurological Institute
3801 University, Suite 778
Montreal, Quebec, Canada H3A 2B4
Tel 514 398 5029
philippe.seguela@mcgill.ca

Number of Figures: 4.
Number of words in Abstract: 217.
Number of words in Introduction: 574.

eNeuro Accepted Manuscript

Number of words in Discussion: 958.

The authors declare no competing financial interests.

This work was supported by grants from the Canadian Institutes of Health Research [MOP-130239], the Natural Sciences and Engineering Council of Canada [DG-203061], the Quebec Pain Research Network and the Louise and Alan Edwards Foundation. ID holds a FRQS doctoral studentship, HB holds FRQS and Arthritis Society postdoctoral fellowships.

eNeuro Accepted Manuscript

Abstract

We report a novel transgenic mouse model in which the terminals of peripheral nociceptors can be silenced optogenetically with high spatio-temporal precision, leading to the alleviation of inflammatory and neuropathic pain. Inhibitory archaerhodopsin-3 (Arch) proton pumps were delivered to $Na_v1.8^+$ primary afferents using the *Na_v1.8-Cre* driver line. Arch expression covered both peptidergic and non-peptidergic nociceptors and yellow light stimulation reliably blocked electrically-induced action potentials in DRG neurons. Acute transdermal illumination of the hind paw of *Na_v1.8-Arch$^+$* mice significantly reduced mechanical allodynia under inflammatory conditions, while basal mechanical sensitivity was not affected by the optical stimulation. Arch-driven hyperpolarization of nociceptive terminals was sufficient to prevent ChR2-mediated mechanical and thermal hypersensitivity in double transgenic *Na_v1.8-ChR2$^+$-Arch$^+$* mice. Furthermore, prolonged optical silencing of peripheral afferents in anesthetized *Na_v1.8-Arch$^+$* mice led to post-stimulation analgesia with a significant decrease in mechanical and thermal hypersensitivity under inflammatory and neuropathic conditions. These findings highlight the role of peripheral neuronal inputs in the onset and maintenance of pain hypersensitivity, demonstrate the plasticity of pain pathways even after sensitization has occurred, and support the involvement of $Na_v1.8^+$ afferents in both inflammatory and neuropathic pain. Taken together, we present a selective analgesic approach in which genetically-identified subsets of peripheral sensory fibers can be remotely and optically inhibited with high temporal resolution, overcoming the compensatory limitations of genetic ablations.

eNeuro Accepted Manuscript

Significance statement

Selective activation and/or inhibition of peripheral nociceptors allow us to control pain transmission and modulate pain perception. Here, we generated a novel transgenic mouse line in which optical activation of archaerhodopsin-3 (Arch) proton pumps efficiently silenced the activity of $Na_v1.8^+$ nociceptive afferents. Acute and prolonged transdermal illumination of the hind paws of *$Na_v1.8$-Arch$^+$* mice reduced mechanical and thermal hypersensitivity under inflammatory and neuropathic conditions, underlining the contribution of the peripheral neuronal component, particularly $Na_v1.8^+$ fibers, in the transmission of evoked pain as well as the development and maintenance of chronic pain. This optogenetic approach can be applied to functionally investigate other subsets of sensory neurons with high temporal precision, and safe genetic delivery of inhibitory opsins may prove useful for clinical applications.

eNeuro Accepted Manuscript

84 **Introduction**

85 Nociceptors are the primary transducers of noxious and/or potentially damaging stimuli from the
86 periphery to the central nervous system. $Na_v1.8$ is a voltage-gated sodium channel expressed in this
87 subpopulation of primary sensory neurons (Shields et al., 2012). $Na_v1.8$ channels play an important role
88 in the generation and propagation of action potentials; thus, altering their activity affects neuronal
89 excitability (Garrison et al., 2014; Han et al., 2016). Moreover, $Na_v1.8$-expressing neurons have been
90 identified as major players in pain onset and hypersensitivity under chronic conditions.
91 Pharmacological and genetic tools have been used to either interfere with $Na_v1.8$ channel functionality
92 (Laird et al., 2002; Gaida et al., 2005; Jarvis et al., 2007; Yu et al., 2011) or to ablate the $Na_v1.8^+$
93 population in order to assess its role in a variety of pain conditions (Abrahamsen et al., 2008). These
94 studies confirmed the involvement of this neuronal population in pain hypersensitivity under
95 inflammatory conditions, while its role in neuropathic pain has remained controversial (Gaida et al.,
96 2005; Nassar et al., 2005; Villarreal et al., 2005; Joshi et al., 2006; Jarvis et al., 2007; Abrahamsen et
97 al., 2008; Yu et al., 2011).

98 Pharmacological approaches lack temporal control over drug activity, and target selectivity is a
99 challenge due to the high homology between subtypes of voltage-gated sodium channels. Genetic tools
100 such as knockouts and ablation strategies do not account for compensation at the cellular and circuit
101 levels.

102 An optogenetic approach might fill these gaps ensuring a precise spatiotemporal control of the activity
103 of $Na_v1.8$-expressing neurons and allowing a peripheral interference with nociceptive transduction. In
104 rats, expression of archaerhodopsin (ArchT) pumps in the fast-conducting myelinated A-δ high
105 threshold mechanoreceptors allowed the silencing of these fibers, showing their involvement in
106 withdrawal behaviors under normal and neuropathic (pSNL) conditions (Boada et al., 2014). In mice,
107 optical activation of ArchT pumps, expressed under the control of the TRPV1 promoter, resulted in
108 reduced mechanical and thermal sensitivities under normal conditions (Li et al., 2015). However, the

eNeuro Accepted Manuscript

latter study did not investigate the analgesic effect of ArchT activation under chronic pain conditions. In another study, following viral delivery of halorhodopsin (NpHR) pumps to a subset of small diameter C-fiber neurons, transdermal yellow light illumination increased sensory thresholds under normal conditions and decreased pain hypersensitivity caused by chronic constriction injury (CCI) (Iyer et al., 2014). Yet, NpHR-mediated analgesia was only assessed in the CCI model, and the neuronal population transduced by the virus was not genetically defined.

Based on the *Na_v1.8-ChR2*$^+$ mouse model (Daou et al., 2013) using the *Na_v1.8-Cre* knock-in construct (Stirling et al., 2005), we specifically delivered inhibitory opsins to $Na_v1.8^+$ neurons to silence the activity of their peripheral terminals with high temporal precision, assess their involvement in several pain conditions without any ablation, and validate the analgesic potential of optogenetic actuators. Following the functional assessment of Arch pumps *in vitro*, acute and prolonged transdermal yellow light stimulation of the hind paws of *Na_v1.8-Arch*$^+$ mice were used to evaluate Arch-mediated analgesia under inflammatory and neuropathic conditions. Our results show that acute blockade of $Na_v1.8^+$ terminals reduces pain transmission and prolonged inhibition of peripheral input causes short-term analgesia outlasting the optical stimulation. Both strategies support the involvement of $Na_v1.8^+$ afferents in inflammatory and neuropathic pain, and the latter highlights the plasticity of the nociceptive circuit under sensitized conditions. This optogenetic approach provides useful tools to interrogate specific components of the peripheral sensory pathways as well as a promising basis for gene therapy to treat chronic pain.

eNeuro Accepted Manuscript

Materials and Methods

Subjects and mouse lines

Five to sixteen weeks old C57BL/6 mice of both sexes, weighing 20–35g, were used in this study. All animal procedures were performed in accordance with the authors' University Animal Care Committee's regulations. Homozygous *Na_v1.8-Cre* mice (Stirling et al., 2005) were crossed with homozygous Ai35 mice (Jackson Laboratory) carrying the *floxed stop-Arch-EGFP* gene in the *ROSA26* locus (Madisen et al., 2012), to generate the *Na_v1.8-Arch$^+$* mouse line. Similarly, mice carrying *Tau-EGFP* in the *ROSA26* locus (Dr. Ulrich Boehm, University of Hamburg, Germany) were crossed with homozygous *Na_v1.8-Cre* mice to generate *Na_v1.8-Tau$^+$* control mice. Heterozygous *Na_v1.8-ChR2$^+$* mice were crossed with homozygous Ai35 mice to generate the *Na_v1.8-ChR2$^+$-Arch$^+$* double transgenic mouse line.

Immunofluorescence

Mice were intracardially perfused with 50 mL saline (0.9% NaCl), followed by 200 mL of 4% paraformaldehyde (PFA) in 0.01 M phosphate buffered saline (PBS), pH 7.4, at room temperature for 30 min. Dorsal root ganglia (DRG), spinal cord, and glabrous skin were extracted and post-fixed in 4% PFA for 24 h at 4 ^{o}C. Tissue was then cryoprotected in 30% sucrose in PBS overnight at 4 ^{o}C. To study the spinal cord and glabrous skin, 40 µm-thick sections were cut at -20 ^{o}C using a cryostat (Leica). All sections were collected as free-floating in PBS containing 0.2% Triton-X 100 (PBS-T). As for the DRG, sectioning at 14 µm thickness was performed directly onto gelatin-subbed slides. Sections were initially permeabilized with 50% ethanol for 30 min followed by 1 min incubation in a 0.3% hydrogen peroxide solution. Sections were washed in PBS-T for 30 min between all incubations. Nonspecific binding of the secondary antibody was blocked by pre-treating the sections for 1 h at room temperature in 10% normal goat and donkey serum (Gibco, Carlsbad, CA) diluted in PBS. The sections were then incubated at 4 °C for 24 h with a rabbit anti-Calcitonin Gene Related Protein (CGRP) antibody (Sigma)

eNeuro Accepted Manuscript

and a guinea pig anti-purinoceptor P2X3 antibody (Neuromics) at a dilution of 1:2000 and 1:25000, respectively. After several rinses in PBS-T, sections were incubated for 90 min at room temperature with a biotin-conjugated donkey anti-guinea pig IgG (1:200; Jackson ImmunoResearch Laboratories) in PBS, followed by further signal amplification via tyramide (1:75; PerkinElmer) for 7 min. The sections were incubated for 2 h at room temperature with a mixture of Streptavidin conjugated to Alexa Fluor 568 (1:200; Molecular Probes) and highly cross-adsorbed goat anti-rabbit IgG conjugated to Alexa Fluor 647 (1:800; Molecular Probes) in 5% normal goat and donkey serum in PBS-T. Finally, the sections were washed, mounted on gelatin-subbed slides (spinal cord and glabrous skin), air-dried and cover slipped with anti-fading mounting medium (Aqua PolyMount, Polysciences). Slides were stored at 4 °C until examination under a Zeiss LSM 710 confocal microscope.

Cell culture and DRG preparation

DRG were extracted from adult *Na_v1.8-Arch$^+$* mice or adult *Na_v1.8-ChR2$^+$-Arch$^+$* mice and kept in sterile ice-cold 1x HBSS Hanks medium (Gibco) throughout the dissection. DRG were then incubated in 5 mL HBSS containing 1.4 mg/mL dispase (Sigma-Aldrich) and 1.1 mg/mL collagenase type II (Sigma-Aldrich) for 45 min at 37 ^{o}C. Following the enzymatic reaction, DRG were washed twice with 10 mL of culture media (F-12 media (Gibco), containing 10% FBS, 1% L-Glutamine, 1% Penicillin, and 1% Streptomycin) and then mechanically triturated using fire-polished Pasteur pipettes. The dissociated neurons were finally plated onto five 35 mm culture dishes (Starsted, 2 mL/dish) previously coated with laminin (BD Bioscience) and poly-D-lysine (Sigma-Aldrich). Cells were incubated for 24 h at 37 ^{o}C and 5% CO_2 prior to electrophysiological recording.

Whole-cell electrophysiology

Whole-cell patch clamp recordings on DRG neurons were conducted at room temperature, 24 h post-plating. The pipette's internal solution (pH 7.2) contained in mM: 130 K-gluconate, 1 $MgCl_2$, 10

eNeuro Accepted Manuscript

HEPES, 5 EGTA, 3 MgATP, and 0.4 GTP. Bath solution (pH 7.4) contained in mM: 152 NaCl, 5 KCl, 2 $CaCl_2$, 1 $MgCl_2$, 10 HEPES, and 10 glucose. Patch pipettes had a tip resistance of 5–10 MΩ. Electrophysiological recordings were conducted using an Axopatch 200B amplifier, digitized with a Digidata 1322A interface (Axon Instruments, Foster City, CA.). Traces were acquired and analyzed using pClamp 8.2 software (Axon Instruments). Recordings were low-pass filtered at 2 KHz and 5 KHz in voltage and current clamp configurations, respectively. Multimode optic fibers (200 µm diameter, Thorlabs), coupled to DPSS lasers of specific wavelengths (473 nm blue laser, Laserglow Technologies, Canada or 589 nm yellow laser, Dragon Lasers, China), were used for optical stimulation of DRG neurons. Stimulation parameters are specified in each condition. Light intensities were measured using a PM100A power meter coupled to a S130C photodiode sensor (Thorlabs) and analyzed using LabVIEW 8.5 software.

Behavioral experiments under normal and inflammatory conditions

Due to the nature of the experiments, particularly the use of visible light, trials were not conducted blindly. Mice were habituated for 1 h prior to testing. Thermal sensitivity was measured using the radiant heat paw-withdrawal test. A blue filter (True Blue #196; Lee Filters) was placed on the light source to filter out the orange-yellow component and prevent non-specific activation of Arch pumps. Mechanical sensitivity was assessed using an automated von Frey fiber (UgoBasile dynamic plantar aesthesiometer) applied to the mid-plantar hind paw. The non-treated hind paw was used as a control.

The analgesic effect of acute optical stimulation was assessed under normal and inflammatory conditions. Yellow light was applied to the plantar surface of the hind paw simultaneously with the mechanical or thermal stimulus. The light was administered continuously using a 1 mm optic fiber (Prizmatix) coupled to a 589 nm laser.

Two inflammatory conditions were used to assess the effect of yellow light stimulation on mechanical hypersensitivity in $Na_v1.8\text{-}Arch^+$ mice: an intradermal injection of 10 µl capsaicin (0.05%, Sigma) into

eNeuro Accepted Manuscript

the right hind paw, leading to mechanical allodynia lasting at least 60 min post-injection, and an intraplantar injection of 20 µl zymosan (1 mg/ml, Sigma) into the left hind paw, leading to mechanical allodynia lasting up to 24 h post-injection. Control *Na_v1.8-Arch*$^+$ mice were injected with inflammatory compounds but no optical stimulation was applied while assessing mechanical sensitivity.

To test the effect of prolonged silencing of $Na_v1.8^+$ fibers on inflammatory pain, mechanical and thermal sensitivities were assessed before and after a prolonged (1 h) yellow light stimulation of the injected hind paw. The hour-long stimulations were conducted under 2% isoflurane anesthesia with a 3 s ON, 1 s OFF pulsing frequency. The light beam (0.3-0.45 mW/mm^2) covered the entire plantar surface. Control *Na_v1.8-Arch*$^+$ mice were injected with the inflammatory compound and placed under isoflurane for 1 h without any optical stimulation. Mechanical and thermal measurements were taken at least 1 h post-stimulation to give the mice enough time to recover from anesthesia. An intraplantar injection of 20 µl zymosan (1 mg/ml) was used to investigate the mechanical modality, while an intraplantar injection of 25 µl emulsified Complete Freund's Adjuvant (CFA, 0.5 mg/ml, EMD Millipore) was used to study the thermal modality, because CFA produced more consistent and reproducible thermal hypersensitivity than zymosan. Zymosan-induced mechanical hypersensitivity was measured 2, 4, 6, 8 and 24 h post-injection while CFA-mediated thermal hypersensitivity was assessed 2, 24, 48, and 72 h post-injection.

Behavioral testing on the double-opsin mouse line

To determine whether yellow light can prevent blue light-induced ChR2-mediated hypersensitivity, the left hind paw of *Na_v1.8-ChR2*$^+$*-Arch*$^+$ mice was stimulated either with blue light alone or with blue and yellow light simultaneously (blue: 2 Hz at 2.3 mW/mm^2, yellow: 3 s ON 1 s OFF at 0.3-0.45 mW/mm^2; 30 min for mechanical, 1 h for thermal). Thermal and mechanical sensitivities were measured before, and 1, 3, and 24 h post-stimulation. All stimulations were done under isoflurane anesthesia, right hind paws were used as controls.

eNeuro Accepted Manuscript

Spared nerve injury and mechanical allodynia

Six weeks old mice were deeply anesthetized using 2% isoflurane. The left anterior thigh of the animal was shaved and disinfected using 70% isopropyl alcohol. To induce the SNI neuropathy, an incision was made through the anterior surface of the left thigh to expose the sciatic nerve at the trifurcation level. The common peroneal and tibial nerves were tightly ligated with 6.0 silk and sectioned distal to the ligation. The sural nerve was left intact. Sham surgery involved exposing the nerve without damaging it. The skin was closed using interrupted sutures (6.0 silk). A 1 mL subcutaneous saline injection (0.9%) was administered to replenish fluids and the mouse recovered on a heating pad until ambulatory, and was then returned to the cage. An eye ointment (Tears Naturale P.M.) was applied to keep the eyes lubricated during the procedure.

Mechanical sensitivity of both hind paws was measured up to 9 weeks post-surgery, using von Frey monofilaments (Stoelting). Monofilaments allow the precise targeting of the lateral part of the hind paw. At 3, 4, 6 and 9 weeks post-surgery, the neuropathic paw was exposed to a prolonged (1 h, 3 s ON 1 s OFF, 0.3-0.45 mW/mm^2) yellow light stimulation under 2% isoflurane anesthesia. Mechanical sensitivity was measured up to 24 h post-stimulation. To control for the isoflurane effect, neuropathic *Na_v1.8-Arch$^+$* mice were placed under isoflurane for 1 h without optical stimulation. To control for any non-specific yellow light effect, sham *Na_v1.8-Arch$^+$* mice were submitted to the same optical stimulation as the neuropathic mice, and their mechanical sensitivity was followed over a similar time course post-stimulation.

Statistical analysis

All data are represented as mean ± SEM. All statistical tests were performed in GraphPad Prism 6, and statistical significance was set at $p < 0.05$.

eNeuro Accepted Manuscript

For testing under normal conditions, measurements on both hind paws were combined and averaged across animals for each intensity/stimulation paradigm. Comparison was done with the baseline measurements using the paired Student *t*-test (Table 1).

For experiments with the double-opsin mice and all the inflammatory tests (capsaicin, zymosan, CFA), data were averaged for each hind paw at each time point across animals, and comparison was done between the "Ipsi-Light" and "Ipsi-Control" conditions (for inflammatory tests) and between "Ipsi-Blue" and "Ipsi-Blue + Yellow" (for double-opsin experiments) at each time point, using the repeated measures two-way ANOVA test followed by the Sidak post hoc test (Tables 2,3).

Regarding the SNI experiments, data were averaged for each hind paw at each time point across animals, and comparisons were done between the "SNI-Light" and "SNI-Iso" conditions, using the repeated measures two-way ANOVA test followed by the Sidak post-hoc test (Tables 2,3) and between each "Post" time point and "Pre" in the "SNI-Light" group, using the repeated measures one-way ANOVA test followed by the Dunnett post-hoc test (Tables 4,5).

eNeuro Accepted Manuscript

Results

Distribution and functionality of Arch-EGFP in sensory pathways

To assess the expression profile of transgenic Arch-EGFP pumps in the peripheral pathways of *Na_v1.8-Arch*$^+$ mice, we determined their colocalization with the peptidergic and non-peptidergic markers CGRP and P2X3, respectively. In DRG neurons, almost all P2X3- and CGRP-immunopositive cells were EGFP-positive, with the P2X3 and CGRP signals being mutually exclusive (Figure 1A). EGFP fluorescence was further detected in superficial laminae of the dorsal horn of the spinal cord, indicating the efficient trafficking of Arch pumps to their central targets. It colocalized with CGRP labeling in laminae I and II_o and P2X3 labeling in lamina II_i, and extended ventrally to lamina III that is innervated by myelinated fibers (Figure 1B). Transgenic opsins were effectively transported to the periphery, where EGFP fluorescence overlapped with P2X3 and CGRP labeling in the deep and superficial layers of the glabrous skin bordering the dermal-epidermal junction (Figure 1C).

The functionality of Arch-EGFP was then tested in cultured DRG neurons. Typical outward photocurrents (2.04 ± 0.3 pA/pF) were recorded under yellow light (589 nm) stimulation, leading to significant and reproducible membrane hyperpolarizations (-24.15 ± 3.51 mV) (Figure 1D). Light-evoked hyperpolarizations were sufficient to block electrically-induced action potentials in DRG neurons (Figure 1E), showing the ability of Arch pumps to inhibit $Na_v1.8^+$ nociceptors' activity *in vitro*. Taking a closer look at Arch-mediated photocurrents, we detected small inward currents at the beginning of light application (Figure 1D, left panel). However, these ASIC-like currents (Zeng et al., 2015) did not translate into depolarization as shown in the current clamp trace (Figure 1D, right panel). Also, both the size and duration of the depolarizing currents were significantly smaller than the Arch-mediated photocurrents and hyperpolarizations. Altogether, although a decrease in extracellular pH can be depolarizing, the overall effect of optical stimulations is inhibitory.

eNeuro Accepted Manuscript

Analgesic effects of acute optical stimulation *in vivo*

We next tested whether acute optical silencing of $Na_v1.8^+$ afferents interferes with sensory perception in behaving *$Na_v1.8$-Arch*$^+$ mice. Mechanical sensitivity was assessed under normal and inflammatory conditions. Transdermal yellow light illumination of the hind paw was applied simultaneously with the mechanical stimulus. We found that mechanical thresholds were not altered under normal conditions, using a range of light intensities (0.25-0.43 mW/mm^2) (Figure 2A; n = 8–17 mice/condition, paired Student t-test used to compare "No light" vs. "0.25 mW/mm^2" measurements, p = 0.0707[a], Table 1). However, optical stimulation (0.25 mW/mm^2) significantly reduced capsaicin- and zymosan-induced mechanical allodynia (Figure 2B,C; n = 6 mice/condition for capsaicin: comparison between "Ipsi-Light" and "Ipsi-Control" was done using the repeated measures two-way ANOVA test[b], Table 2, followed by the Sidak multiple comparisons test, at 30 min: p = 0.0018[k] and at 60 min: p = 0.0424[k], Table 3. For zymosan, n = 12–13 mice/condition: comparison between "Ipsi-Light" and "Ipsi-Control" was done using the repeated measures two-way ANOVA test[c], Table 2, followed by the Sidak multiple comparisons test, at 2 h: p = <0.0001[l], at 4 h: p = 0.0104[l], and at 6 h: p = 0.0036[l], Table 3), indicating effective Arch-mediated analgesia under inflammatory conditions. These findings are consistent with the role of $Na_v1.8^+$ neurons in mediating inflammatory pain but not in setting basal mechanical sensitivity under normal conditions (Abrahamsen et al., 2008).

The effect of acute yellow light stimulation on the thermal modality was also investigated. Unfortunately, simultaneous application of laser light with the light from the Hargreaves device increased thermal sensitivity in an intensity-dependent manner (data not shown). This was also the case on control *$Na_v1.8$-Tau*$^+$ mice, showing that this effect is Arch-independent (data not shown). This is most likely due to additive heating, making this approach inappropriate to assess Arch-mediated analgesia for the thermal modality.

The analgesic effect observed under inflammation was significant but partial. This can be due to insufficient Arch-driven hyperpolarizations of peripheral afferents to completely block nociceptive

eNeuro Accepted Manuscript

transmission. Alternatively, the absence of Arch expression in subpopulations of sensitized terminals, may explain the partial reversal of mechanical allodynia. For instance, the presence of Arch-negative nociceptors would allow the transduction and transmission of nociceptive inputs from the periphery despite the optical stimulation. Furthermore, low-threshold Aβ mechanoreceptors play an essential role in mediating mechanical allodynia under inflammatory conditions. Thus, the absence of Arch pumps in these fibers enables them to normally transmit mechanical stimuli to the CNS, accounting, at least partially, for the pain hypersensitivity. Another factor that could explain this partial analgesia is a limited penetration of light in the skin, leading to incomplete inhibition of deeper primary afferent terminals. To address these possibilities, we generated the double-opsin *Na_v1.8-ChR2$^+$-Arch$^+$* mice, in which ChR2 channels and Arch pumps are co-expressed in the same $Na_v1.8^+$ neurons, overcoming the limitation of having Arch-negative sensitized terminals. Also, the use of blue light to induce and yellow light to prevent sensitization ensures the targeting of the same afferents since both stimuli have the same physical nature. It has been shown that prolonged blue light stimulation of the hind paw of anesthetized *Na_v1.8-ChR2$^+$* mice induces mechanical as well as thermal hypersensitivity lasting up to 24 h post-stimulation (Daou et al., 2013). Using either blue light alone or blue and yellow light together on *Na_v1.8-ChR2$^+$-Arch$^+$* mice, we assessed the ability of Arch pumps to prevent ChR2-mediated hypersensitivity. When used alone, blue light induced a significant reduction in withdrawal thresholds and latencies lasting up to 24 h; however, this sensitization was completely prevented in presence of yellow light in both mechanical and thermal modalities (Figure 2D,E; for mechanical, n = 6–12 mice/condition: comparison between "Ipsi-Blue" vs. "Ipsi-Blue + Yellow" was done using the repeated measures two-way ANOVA test[d], Table 2, followed by the Sidak multiple comparisons test, at 1 h: p = 0.0034[m] and at 3 h: p = 0.0215[m], Table 3. For thermal, n = 6–13 mice/condition: comparison between "Ipsi-Light" and "Ipsi-Control" was done using the repeated measures two-way ANOVA test[e], Table 2, followed by the Sidak multiple comparisons test, at 1 h: p = 0.0106[n], Table 3). These results are consistent with our *in vitro* recordings in cultured DRG neurons from *Na_v1.8-ChR2$^+$-Arch$^+$* mice, in

eNeuro Accepted Manuscript

which Arch-mediated hyperpolarizations suppressed ChR2-induced action potentials in the same neurons (Figure 2F). These findings support the effectiveness of Arch pumps in silencing peripheral afferents and preventing the onset of sensitization when expressed with high penetrance in the target neurons. Also, the *Na_v1.8-ChR2$^+$-Arch$^+$* mouse line provides a transgenic model in which $Na_v1.8^+$ neurons can be bidirectionally controlled with high spatio-temporal precision.

Prolonged silencing of $Na_v1.8^+$ afferents leads to post-stimulation analgesia

We further tested the effect of a prolonged inhibition of peripheral sensory pathways on inflammatory and neuropathic pain hypersensitivity. Anesthetized *Na_v1.8-Arch$^+$* mice were subjected to hour-long yellow light stimulations at different time points after induction of inflammation or nerve injury. Mechanical thresholds and thermal latencies were measured at least one hour post-light exposure. This approach allowed us to overcome the complications resulting from the simultaneous application of yellow light and thermal stimulus and to assess the analgesic effects of prolonged peripheral silencing.

Under zymosan-induced inflammation, optical stimulation delayed the onset of mechanical allodynia when applied right after injection, while it caused a significant and transient reduction of allodynia when applied 2 and 4 h post-zymosan injection (Figure 3A; *left panel*, n = 7 mice/condition, *middle panel*, n = 7–8 mice/condition, *right panel*, n = 7–11 mice/condition. In all panels, comparison between "Ipsi-Light" and "Ipsi-Control" was done using the repeated measures two-way ANOVA test[f,g,h], Table 2, followed by the Sidak multiple comparisons test: *left panel*, at 2 h: p = 0.0141[o] and at 4 h: p = 0.0128[o], *middle panel*, at 4 h: p = <0.0001[p], *right panel*, at 6 h: p = 0.0007[q], Table 3). In the latter cases, the analgesia peaked at 1 h and returned to control levels 3 h post-optical stimulation.

Arch-mediated analgesia was milder when evaluating thermal hypersensitivity under CFA-induced inflammation. No analgesia was detected when light was applied right after CFA injection, yet, a transitory increase in thermal latencies was measured when light was applied 24 h post-injection (Figure 3B; *right panel*, n = 7 mice/condition, comparison between "Ipsi-Light" and "Ipsi-Control" was

eNeuro Accepted Manuscript

done using the repeated measures two-way ANOVA test[i], Table 2, followed by the Sidak multiple comparisons test, at 24 (+1) h: $p = 0.0331$[r], Table 3). No redness, edema, or any sign of neurogenic inflammation were detected following hour-long stimulations of the hind paw. Furthermore, prolonged exposure to yellow light did not alter thermal sensitivity of naïve *Na_v1.8-Arch*$^+$ mice (Figure 3C). Also, the effect of yellow light under hyperalgesic conditions (CFA) was controlled for using the control transgenic *Na_v1.8-Tau*$^+$ mouse line, where CFA-injected *Na_v1.8-Tau*$^+$ mice were exposed to hour-long light exposure 24-h post-injection. No effects on CFA-mediated thermal hypersensitivity were detected in these mice (data not shown), indicating that the transitory effect observed in *Na_v1.8-Arch*$^+$ mice (Figure 3B, *right panel*) is Arch-mediated.

The partial reversal in both mechanical and thermal modalities can be attributed a) to the possibility that Arch-negative afferents play an important role in the onset and maintenance of pain hypersensitivity, b) to the incomplete blockade of peripheral inputs due to limited light penetration or potency of the stimulus, and/or c) to central sensitization mechanisms independent of peripheral inputs.

To investigate whether Arch pumps desensitize during prolonged optical stimulations, we conducted *in vitro* recordings on cultured DRG neurons from *Na_v1.8-Arch*$^+$ mice, using the same stimulation protocol (3 s ON, 1 s OFF) used *in vivo*. Ten minutes long recordings under sustained optical stimulation showed that Arch-mediated hyperpolarizations are consistent and replicable over time, indicating that a) prolonged illumination does not alter the activity and recovery of Arch pumps (Figure 3D), b) neuronal excitability and input resistance remained unchanged. This further suggests that the analgesic effects observed in behavioral experiments are not due to decreased excitability of peripheral afferents but rather due to central plasticity where blockade of peripheral inputs to the spinal cord reduces central sensitization, leading to decreased pain hypersensitivity.

Using the SNI model to produce a neuropathic condition, we tested whether prolonged inhibition of $Na_v1.8^+$ fibers can reduce mechanical allodynia. Hour-long illuminations of the hind paw markedly decreased mechanical hypersensitivity at 3, 4 and 6 weeks post-SNI surgery, with a transient effect

eNeuro Accepted Manuscript

lasting up to 24 h post-stimulation (Figure 4; n = 7–14 mice for SNI, n = 3–7 mice for Sham. *Left panel*, comparison between "SNI-Iso" vs. "SNI-Light" was done using the repeated measures two-way ANOVA test[j], Table 2, followed by the Sidak multiple comparisons test, at 1 h: $p = 0.0221$[s] and at 2 h: $p = 0.0375$[s], Table 3. Comparison between each "Post" time point and "Pre" in the "SNI-Light" group was conducted using the repeated measures one-way ANOVA test[t], Table 4, followed by the Dunnett multiple comparisons test, at 1 h Post: $p = 0.0093$[v], at 2 h Post: $p = 0.0321$[v], at 2.5 h Post: $p = 0.0181$[v], at 3 h Post: $p = 0.0483$[v], Table 5. *Middle panel*, comparison between each "Post" time point and "Pre" in the "SNI-Light" group was performed using the repeated measures one-way ANOVA test[u], Table 4, followed by the Dunnett multiple comparisons test, at 1 h Post: $p = 0.0437$[w], Table 5). Analgesia was most pronounced at 3 weeks and gradually decreased at 4 and 6 weeks post-SNI (Figure 4). Arch-mediated analgesia was completely lost when optical stimulation was applied 9 weeks post-SNI (data not shown), indicating that peripheral inhibition of $Na_v1.8^+$ nociceptors becomes less efficient in reducing mechanical pain at later stages of neuropathy. By showing that silencing the activity of their peripheral terminals alleviates mechanical allodynia, especially at the early stages of neuropathy, these results clearly demonstrate the involvement of $Na_v1.8^+$ nociceptors in SNI-induced neuropathic pain.

eNeuro Accepted Manuscript

Statistical tables

Table 1. Paired Student *t*-test.

		Data		Test	P
a	Figure 2A	Force (g)	No light vs. 0.25 mW/mm^2	Paired Student *t*-test	0.0707

Table 2. Repeated measures two-way ANOVA.

			Source of Variation											
			Light			Time			Interaction			Matching		
	Data		DFn, DFd	F	P	DFn, DFd	F	P	DFn, DFd	F	P	DFn, DFd	F	P
b	Figure 2B	Force (g)	1,10	9.206	0.0126	2,20	49.6	<0.0001	2,20	4.775	0.0202	10,20	2.371	0.0481
c	Figure 2C	Force (g)	1,23	12.63	0.0017	5,115	44.5	<0.0001	5,115	7.556	<0.0001	23,115	2.298	0.0021
d	Figure 2D	Force (g)	1,16	8.039	0.0119	3,48	7.704	0.0003	3,48	3.194	0.0317	16,48	2.353	0.0115
e	Figure 2E	Latency (s)	1,17	6.192	0.0235	3,51	6.753	0.0006	3,51	2.111	0.1103	17,51	1.418	0.1672
f	Figure 3A Left panel	Force (g)	1,12	11.97	0.0047	5,60	26.74	<0.0001	5,60	2.285	0.0574	12,60	2.566	0.0082
g	Figure 3A Middle panel	Force (g)	1,13	5.769	0.032	5,65	32.44	<0.0001	5,65	4.424	0.0016	13,65	1.016	0.4471
h	Figure 3A Right panel	Force (g)	1,16	0.2823	0.6025	5,80	68.17	<0.0001	5,80	4.293	0.0016	16,80	1.734	0.0567
i	Figure 3B Right panel	Latency (s)	1,12	0.5795	0.4612	8,96	63.15	<0.0001	8,96	2.216	0.0327	12,96	1.634	0.0947
j	Figure 4 Left panel	50% threshold (g)	1,19	8.91	0.0076	5,95	1.826	0.1151	5,95	1.861	0.1085	19,95	3.687	<0.0001

Table 3. Multiple comparisons following repeated measures two-way ANOVA.

		Data	Test	P
k	Figure 2B	At 30 min: Ipsi-Light vs. Ipsi-Control	Sidak	0.0018
		At 60 min: Ipsi-Light vs. Ipsi-Control	Sidak	0.0424
l	Figure 2C	At 2 h: Ipsi-Light vs. Ipsi-Control	Sidak	<0.0001
		At 4 h: Ipsi-Light vs. Ipsi-Control	Sidak	0.0104
		At 6 h: Ipsi-Light vs. Ipsi-Control	Sidak	0.0036
m	Figure 2D	At 1 h: Ipsi-Blue vs. Ipsi-Blue + Yellow	Sidak	0.0034
		At 3 h: Ipsi-Blue vs. Ipsi-Blue + Yellow	Sidak	0.0215
n	Figure 2E	At 1 h: Ipsi-Blue vs. Ipsi-Blue + Yellow	Sidak	0.0106
o	Figure 3A	At 2 h: Ipsi-Light vs. Ipsi-Control	Sidak	0.0141
	Left panel	At 4 h: Ipsi-Light vs. Ipsi-Control	Sidak	0.0128
p	Figure 3A Middle panel	At 4 h: Ipsi-Light vs. Ipsi-Control	Sidak	<0.0001
q	Figure 3A Right panel	At 6 h: Ipsi-Light vs. Ipsi-Control	Sidak	0.0007
r	Figure 3B Right panel	At 24 (+1) h: Ipsi-Light vs. Ipsi-Control	Sidak	0.0331
s	Figure 4	At 1 h: SNI-Iso vs. SNI-Light	Sidak	0.0221
	Left panel	At 2 h: SNI-Iso vs. SNI-Light	Sidak	0.0375

eNeuro Accepted Manuscript

Table 4. Repeated measures one-way ANOVA.

	Data		Time			Matching		
			DFn, DFd	F	P	DFn, DFd	F	P
t	Figure 4 Left panel	50% threshold (g)	3.54,46.02	3.783	0.0123	13,65	3.687	0.0002
u	Figure 4 Middle panel	50% threshold (g)	2.142,27.85	3.304	0.0486	13,52	3.288	0.0011

Table 5. Multiple comparisons following repeated measures one-way ANOVA.

	Data		Test	P
v	Figure 4 Left panel	SNI-Light: Pre vs. 1 h Post	Dunnett	0.0093
		SNI-Light: Pre vs. 2 h Post	Dunnett	0.0321
		SNI-Light: Pre vs. 2.5 h Post	Dunnett	0.0181
		SNI-Light: Pre vs. 3 h Post	Dunnett	0.0483
w	Figure 4 Middle panel	SNI-Light: Pre vs. 1 h Post	Dunnett	0.0437

eNeuro Accepted Manuscript

Discussion

Taking advantage of the *Na_v1.8-Cre* mouse line, we delivered the inhibitory pump Arch to $Na_v1.8^+$ afferents, generating a novel transgenic model in which interference with peripheral nociceptive transmission can be optogenetically achieved with high spatiotemporal precision. This silencing strategy allowed us to specifically manipulate the $Na_v1.8^+$ neuronal subpopulation while overcoming the compensatory effects encountered using other genetic strategies such as knockdowns, knockouts or cell ablation.

The $Na_v1.8^+$ population covers peptidergic and non-peptidergic nociceptors as well as a subset of low-threshold mechanoreceptors. Under inflammatory and neuropathic conditions, central sensitization and plasticity as well as disinhibition in the spinal cord occur; input from low-threshold Aβ fibers can now be relayed to nociceptive circuits in the dorsal horn leading to pain perception. This phenomenon accounts, at least partially, for the mechanical allodynia in chronic pain conditions. Thus, optogenetic silencing of $Na_v1.8^+$ myelinated A-fibers would further reduce pain hypersensitivity, which is in accordance with the analgesic effects we observe.

Acute yellow light illumination of the hind paws of *Na_v1.8-Arch$^+$* mice did not alter their mechanical thresholds under normal conditions. These results fit with those showing that von Frey thresholds were unaffected when the whole $Na_v1.8^+$ subpopulation of neurons was eliminated (Abrahamsen et al., 2008), indicating that these neurons are not essential in setting basal mechanical sensitivity. The same transdermal optical stimulation reduced mechanical allodynia induced by capsaicin and zymosan, demonstrating that a brief and acute silencing of $Na_v1.8^+$ fibers is sufficient to alleviate inflammatory pain. Furthermore, a prolonged inhibition of $Na_v1.8^+$ afferents delayed the onset and/or transiently reduced inflammatory mechanical allodynia. This shows that Arch-mediated inhibition of the terminals of peripheral nociceptors is effective in decreasing inflammatory pain, confirming the involvement of the $Na_v1.8^+$ subpopulation in mediating hypersensitivity under inflammatory conditions. The mechanisms of inhibition in the two stimulation protocols may be different: under acute light

eNeuro Accepted Manuscript

stimulation, analgesia may be mediated by direct hyperpolarization of the sensory fiber(s) transducing the mechanical stimulus since both stimuli are applied simultaneously; following long illumination, synaptic changes in the spinal circuitry may occur due to peripheral silencing of nociceptive inputs, leading to decreased central sensitization and reduced allodynia. Hour-long yellow light stimulations of CFA-injected *$Na_v1.8$-Arch$^+$* mice led to transitory increase in thermal latencies when applied 24 h post-injection but not right after injection. These findings indicate that Arch pumps are not capable of blocking or delaying the onset of CFA-induced thermal hyperalgesia. This apparent discrepancy with the zymosan results might be explained by the difference in the sensory modality investigated or by the strength of the CFA stimulation that could not be reversed as effectively.

Under neuropathic conditions, the role of $Na_v1.8^+$ neurons remained unclear (Nassar et al., 2005; Joshi et al., 2006; Jarvis et al., 2007; Abrahamsen et al., 2008). Using the SNI model, we showed that prolonged hyperpolarization of $Na_v1.8^+$ afferents produces a significant and transient alleviation of mechanical allodynia at 3 and 4 weeks post-surgery, proving the contribution of the $Na_v1.8^+$ population and demonstrating the analgesic effectiveness of our optogenetic strategy in neuropathic pain. Analgesia may be explained by Arch-mediated blockade of the spontaneous hyperactivity of peripheral nociceptors presumably leading to a modified sensitivity of their terminals and/or altered spinal connectivity affecting central sensitization. Interestingly, the analgesic effect of yellow light decreased over time post-surgery, suggesting that peripheral inputs in general, specifically inputs from the $Na_v1.8^+$ population, are not essential for the maintenance of mechanical allodynia.

Arch pumps extrude protons from the cell. This can lead to changes in intracellular and/or extracellular pH affecting neuronal activity. Previous reports have shown that changes in intracellular pH (pH_i) following Arch activation in cultured neurons do not exceed 0.1-0.15 units. Alkalinization of the intracellular space is very limited most likely due to intrinsic stabilization mechanisms in the neuron (such as transporters, exchangers) preventing the development of proton gradients and further increase in pH_i (Chow et al., 2010; Chow et al., 2012). Furthermore, during *in vivo* recordings in mice and

eNeuro Accepted Manuscript

macaques, spike waveform and frequency were not affected before and after prolonged (several minutes) Arch-mediated inhibition (Chow et al., 2012). Extracellularly, proton efflux can lead to a transient decrease in pH and therefore activation of proton-gated channels. A recent study showed that Arch activation induces ASIC currents in HEK293 cells and cortical neurons overexpressing ASIC1a. This was detected as an inward deflection in voltage clamp recordings *in vitro* under green light illumination (Zeng et al., 2015). These inward currents were also detected in our DRG recordings under yellow light stimulation, yet their amplitudes were smaller and did not cause any significant depolarization. This difference in current size is normal since the levels of expression of endogenous acid-sensitive channels are lower than those observed in overexpression systems. Thus, although decrease in extracellular pH can be sensitizing for peripheral terminals, the overall effect of the optical stimulations is analgesic, indicating that the inhibitory component of Arch activation overcomes any sensitizing or excitatory effect of transient acid-evoked currents.

In conclusion, the *Na_v1.8-Arch*$^+$ mouse line represents a constitutive model in which silencing of peripheral nociceptors is achieved remotely with high spatio-temporal precision. We can predict that such an optogenetic approach will be implemented using next-generation inhibitory opsins such as ChloC (Wietek et al., 2014) or the newly identified *Gt*ACR anion channels (Govorunova et al., 2015), possibly leading to more pronounced analgesia. Moreover, considering the large heterogeneity of sensory neurons revealed by recent molecular profiling studies (Goswami et al., 2014; Flegel et al., 2015; Usoskin et al., 2015), our silencing strategy will be beneficial for selective targeting and functional interrogation of other subsets of sensory neurons, including non-nociceptive populations. Selective delivery of inhibitory opsins to genetically-identified neurons will allow the control of pain circuits *in vivo*, setting the stage for a potential use in humans for the treatment of intractable chronic pain.

eNeuro Accepted Manuscript

540 **References**
541

542 Abrahamsen B, Zhao J, Asante CO, Cendan CM, Marsh S, Martinez-Barbera JP, Nassar MA,
543 Dickenson AH, Wood JN (2008) The cell and molecular basis of mechanical, cold, and
544 inflammatory pain. Science 321:702-705.

545 Boada MD, Martin TJ, Peters CM, Hayashida K, Harris MH, Houle TT, Boyden ES, Eisenach JC, Ririe
546 DG (2014) Fast-conducting mechanoreceptors contribute to withdrawal behavior in normal and
547 nerve injured rats. Pain 155:2646-2655.

548 Chow BY, Han X, Boyden ES (2012) Genetically encoded molecular tools for light-driven silencing of
549 targeted neurons. Prog Brain Res 196:49-61.

550 Chow BY, Han X, Dobry AS, Qian X, Chuong AS, Li M, Henninger MA, Belfort GM, Lin Y,
551 Monahan PE, Boyden ES (2010) High-performance genetically targetable optical neural
552 silencing by light-driven proton pumps. Nature 463:98-102.

553 Daou I, Tuttle AH, Longo G, Wieskopf JS, Bonin RP, Ase AR, Wood JN, De Koninck Y, Ribeiro-da-
554 Silva A, Mogil JS, Seguela P (2013) Remote optogenetic activation and sensitization of pain
555 pathways in freely moving mice. J Neurosci 33:18631-18640.

556 Flegel C, Schobel N, Altmuller J, Becker C, Tannapfel A, Hatt H, Gisselmann G (2015) RNA-Seq
557 Analysis of Human Trigeminal and Dorsal Root Ganglia with a Focus on Chemoreceptors. PloS
558 one 10:e0128951.

559 Gaida W, Klinder K, Arndt K, Weiser T (2005) Ambroxol, a Nav1.8-preferring Na(+) channel blocker,
560 effectively suppresses pain symptoms in animal models of chronic, neuropathic and
561 inflammatory pain. Neuropharmacology 49:1220-1227.

562 Garrison SR, Weyer AD, Barabas ME, Beutler BA, Stucky CL (2014) A gain-of-function voltage-
563 gated sodium channel 1.8 mutation drives intense hyperexcitability of A- and C-fiber neurons.
564 Pain 155:896-905.

eNeuro Accepted Manuscript

565 Goswami SC, Mishra SK, Maric D, Kaszas K, Gonnella GL, Clokie SJ, Kominsky HD, Gross JR,
566 Keller JM, Mannes AJ, Hoon MA, Iadarola MJ (2014) Molecular signatures of mouse TRPV1-
567 lineage neurons revealed by RNA-Seq transcriptome analysis. J Pain 15:1338-1359.
568 Govorunova EG, Sineshchekov OA, Janz R, Liu X, Spudich JL (2015) NEUROSCIENCE. Natural
569 light-gated anion channels: A family of microbial rhodopsins for advanced optogenetics.
570 Science 349:647-650.
571 Han C, Huang J, Waxman SG (2016) Sodium channel Nav1.8: Emerging links to human disease.
572 Neurology Jan 8 (Epub).
573 Iyer SM, Montgomery KL, Towne C, Lee SY, Ramakrishnan C, Deisseroth K, Delp SL (2014) Virally
574 mediated optogenetic excitation and inhibition of pain in freely moving nontransgenic mice.
575 Nat Biotech 32:274-278.
576 Jarvis MF et al. (2007) A-803467, a potent and selective Nav1.8 sodium channel blocker, attenuates
577 neuropathic and inflammatory pain in the rat. PNAS 104:8520-8525.
578 Joshi SK, Mikusa JP, Hernandez G, Baker S, Shieh CC, Neelands T, Zhang XF, Niforatos W, Kage K,
579 Han P, Krafte D, Faltynek C, Sullivan JP, Jarvis MF, Honore P (2006) Involvement of the
580 TTX-resistant sodium channel Nav 1.8 in inflammatory and neuropathic, but not post-operative,
581 pain states. Pain 123:75-82.
582 Laird JM, Souslova V, Wood JN, Cervero F (2002) Deficits in visceral pain and referred hyperalgesia
583 in Nav1.8 (SNS/PN3)-null mice. J Neurosci 22:8352-8356.
584 Li B, Yang XY, Qian FP, Tang M, Ma C, Chiang LY (2015) A novel analgesic approach to
585 optogenetically and specifically inhibit pain transmission using TRPV1 promoter. Brain Res
586 1609:12-20.
587 Madisen L et al. (2012) A toolbox of Cre-dependent optogenetic transgenic mice for light-induced
588 activation and silencing. Nat Neurosci 15:793-802.

eNeuro Accepted Manuscript

589 Nassar MA, Levato A, Stirling LC, Wood JN (2005) Neuropathic pain develops normally in mice
590 lacking both Na(v)1.7 and Na(v)1.8. Mol Pain 1:24.
591 Shields SD, Ahn HS, Yang Y, Han C, Seal RP, Wood JN, Waxman SG, Dib-Hajj SD (2012) Na(v)1.8
592 expression is not restricted to nociceptors in mouse peripheral nervous system. Pain.
593 Stirling LC, Forlani G, Baker MD, Wood JN, Matthews EA, Dickenson AH, Nassar MA (2005)
594 Nociceptor-specific gene deletion using heterozygous NaV1.8-Cre recombinase mice. Pain
595 113:27-36.
596 Usoskin D, Furlan A, Islam S, Abdo H, Lonnerberg P, Lou D, Hjerling-Leffler J, Haeggstrom J,
597 Kharchenko O, Kharchenko PV, Linnarsson S, Ernfors P (2015) Unbiased classification of
598 sensory neuron types by large-scale single-cell RNA sequencing. Nat Neurosci 18:145-153.
599 Villarreal CF, Sachs D, Cunha FQ, Parada CA, Ferreira SH (2005) The role of Na(V)1.8 sodium
600 channel in the maintenance of chronic inflammatory hypernociception. Neurosci Lett 386:72-
601 77.
602 Wietek J, Wiegert JS, Adeishvili N, Schneider F, Watanabe H, Tsunoda SP, Vogt A, Elstner M,
603 Oertner TG, Hegemann P (2014) Conversion of channelrhodopsin into a light-gated chloride
604 channel. Science 344:409-412.
605 Yu YQ, Zhao F, Guan SM, Chen J (2011) Antisense-mediated knockdown of Na(V)1.8, but not
606 Na(V)1.9, generates inhibitory effects on complete Freund's adjuvant-induced inflammatory
607 pain in rat. PloS one 6:e19865.
608 Zeng WZ, Liu DS, Liu L, She L, Wu LJ, Xu TL (2015) Activation of acid-sensing ion channels by
609 localized proton transient reveals their role in proton signaling. Scient Rep 5:14125.

610
611
612
613

eNeuro Accepted Manuscript

Figure Legends

Figure 1. Distribution and functionality of Arch-EGFP pumps in the peripheral sensory pathways of *Na_v1.8-Arch*$^+$ mice.

Confocal micrographs showing the fluorescence of Arch-EGFP (green), CGRP immunostaining (blue), P2X3 labeling (red), and the merge. ***A***, Arch-EGFP colocalizes with either P2X3 or CGRP in dorsal root ganglia neurons, validating its selective expression in nociceptors. ***B***, Arch-EGFP fluorescence overlaps with CGRP and P2X3 labeling in laminae I and II of the dorsal horn of spinal cord. ***C***, Arch-EGFP colocalizes with CGRP and P2X3 in free nerve endings in the lower and upper dermis of glabrous skin. Insets at lower magnification (20X). Scale bars, 50 µm. ***D***, Representative yellow (589 nm) light-induced outward photocurrent and membrane hyperpolarization in a DRG neuron. Magnification shows an inward deflection in the voltage clamp trace (arrow), illustrating a proton-mediated ASIC-like current. This inward current did not translate into a depolarization in the current clamp trace. ***E***, Arch-mediated blockade of electrically-induced action potentials (10 ms, 0.4 nA current injection) in DRG neurons. Optical stimulation was continuous (intensity = 0.83 mW/mm^2). V_h= -60 mV in voltage clamp and the resting membrane potential was -62.23 ± 2.92 mV in current clamp configuration (*n* = 8–9 cells).

Figure 2. Analgesic effect of acute yellow light stimulation under normal and inflammatory conditions in *Na_v1.8-Arch*$^+$ mice, and under prolonged blue light stimulation in *Na_v1.8-ChR2*$^+$-*Arch*$^+$ mice.

A, Mechanical sensitivity of *Na_v1.8-Arch*$^+$ mice under normal conditions, using different yellow light (589 nm) intensities (*n* = 8–17 mice/condition, paired Student *t*-test used to compare "No light" vs. 0.25 mW/mm^2 measurements, p = 0.0707[a], Table 1). ***B, C***, Optical stimulation reduced mechanical allodynia under capsaicin- and zymosan- induced inflammation. Yellow light (0.25 mW/mm^2) was

eNeuro Accepted Manuscript

applied to the hind paw of *Na_v1.8-Arch*$^+$ mice simultaneously with the mechanical stimulus at each time point post-injection (*n* = 6–13 mice/condition). ***D, E***, Simultaneous application of yellow and blue light to the hind paw of *Na_v1.8-ChR2*$^+$*-Arch*$^+$ mice prevented the development of blue light-induced mechanical (***D***) and thermal (***E***) hypersensitivity. Post-treatment measurements were taken without any optical stimulation (*n* = 6–13 mice/condition). Symbols represent mean ± SEM of hind paw withdrawal thresholds and latencies before (Pre) and after (Post) treatment. Data were analyzed using the repeated measures two-way ANOVA test followed by Sidak post-hoc test. Significance (*) is reported between "Ipsi-Light" and "Ipsi-Control" (panels ***B***, ***C***) and between "Ipsi-Blue" and "Ipsi-Blue + Yellow" (panels ***D***, ***E***). *$p < 0.05$, **$p < 0.01$, ****$p < 0.0001$. ***F***, Representative yellow (589 nm) and blue (473 nm) light-induced photocurrents in DRG neurons from *Na_v1.8-ChR2*$^+$*-Arch*$^+$ mice. Arch-mediated membrane hyperpolarization was sufficient to block ChR2-induced action potentials (50 ms pulses) in the same neuron (*n* = 4–5 cells). Light intensity was 0.78 mW/mm^2 (blue) and 0.83 mW/mm^2 (yellow).

Figure 3. Analgesic effect of prolonged yellow light stimulation under inflammatory conditions in *Na_v1.8-Arch*$^+$ mice.

Orange bars represent the hour-long yellow light stimulations. ***A***, Prolonged silencing of $Na_v1.8^+$ fibers led to post-stimulation analgesia, reducing zymosan-mediated mechanical allodynia. Optical stimulation was done right after, 2-h Post, and 4-h Post zymosan injection (*n* = 7–11 mice/condition). ***B***, Prolonged yellow light stimulation reduced CFA-induced thermal hypersensitivity when applied 24-h Post CFA injection but not right after (*n* = 5–7 mice/condition). ***C***, Hour-long stimulation does not affect thermal sensitivity in naïve *Na_v1.8-Arch*$^+$ mice (*n* = 6 mice). ***D***, Representative traces showing consistent and reproducible Arch-mediated hyperpolarizations in cultured DRG neurons at 1 and 10 min during a sustained 3 s ON, 1 s OFF stimulation protocol (*n* = 3 cells). Symbols represent mean ± SEM of hind paw withdrawal thresholds and latencies before (Pre) and after (Post) treatment. (*) Significance between "Ipsi-Light" and "Ipsi-Control" measured using the repeated measures two-way

eNeuro Accepted Manuscript

ANOVA test followed by Sidak post-hoc test. *$p < 0.05$, ***$p < 0.001$, ****$p < 0.0001$.

Figure 4. Analgesic effect of prolonged optical stimulation under neuropathic conditions in *$Na_v1.8$-Arch*$^+$ mice.

Orange bars represent the hour-long optical stimulations. Prolonged yellow light application on the neuropathic hind paw decreased SNI-induced mechanical allodynia, showing partial analgesia lasting up to 24 h Post-stimulation, at 3-weeks, 4-weeks and 6-weeks post-SNI surgery (n = 7–14 mice for SNI, n = 3–7 mice for Sham). Symbols represent mean ± SEM of hind paw withdrawal thresholds before (Pre) and after (Post) treatment. (*) Significance between "SNI-Light" and "SNI-Iso", measured using the repeated measures two-way ANOVA test followed by Sidak post-hoc test. *$p < 0.05$. (#) Significance between each "Post" time point and "Pre" in the "SNI-Light" group, measured using the repeated measures one-way ANOVA test followed by Dunnett post-hoc test. # $p < 0.05$, ## $p < 0.01$.

eNeuro Accepted Manuscript

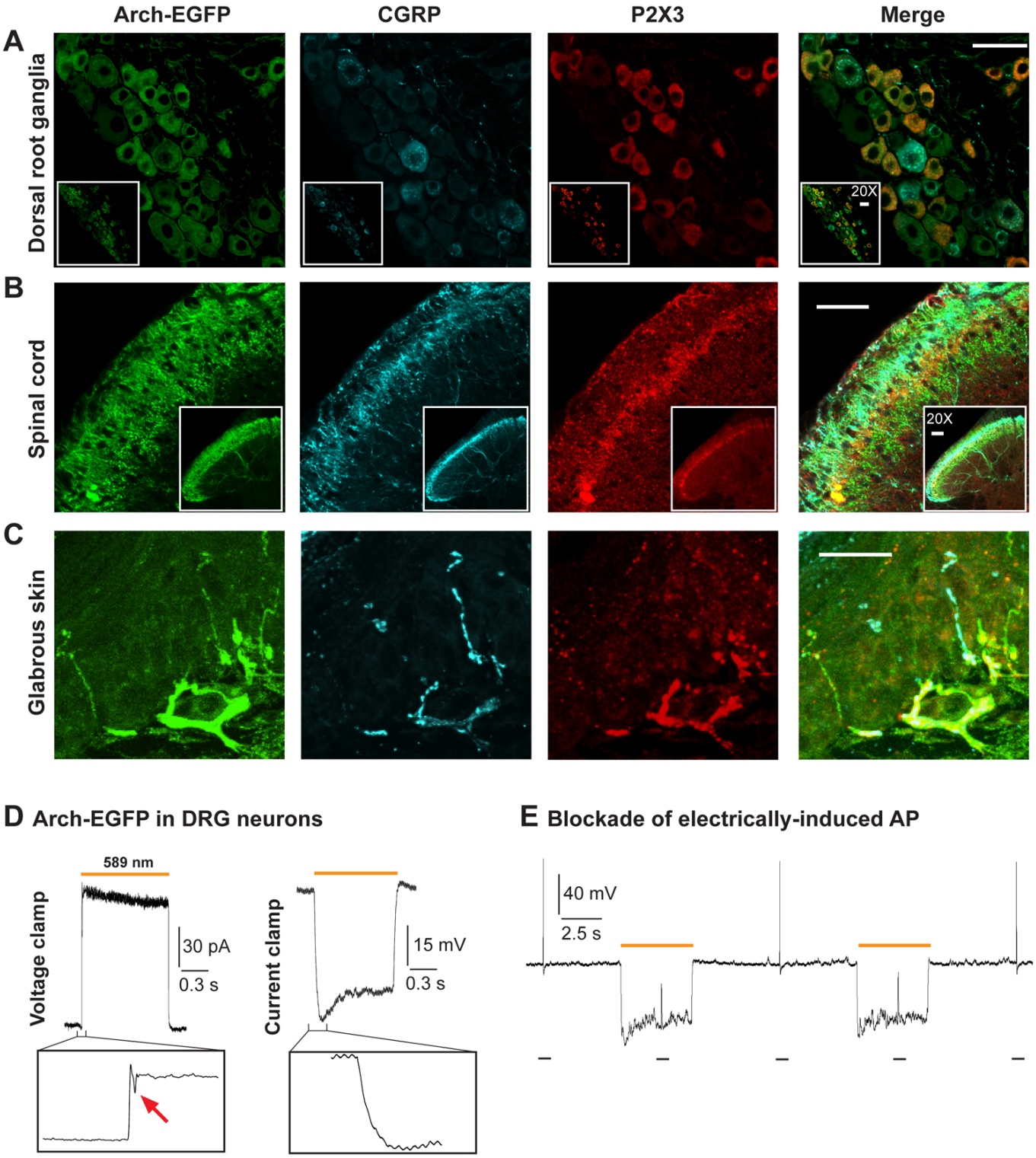

eNeuro Accepted Manuscript

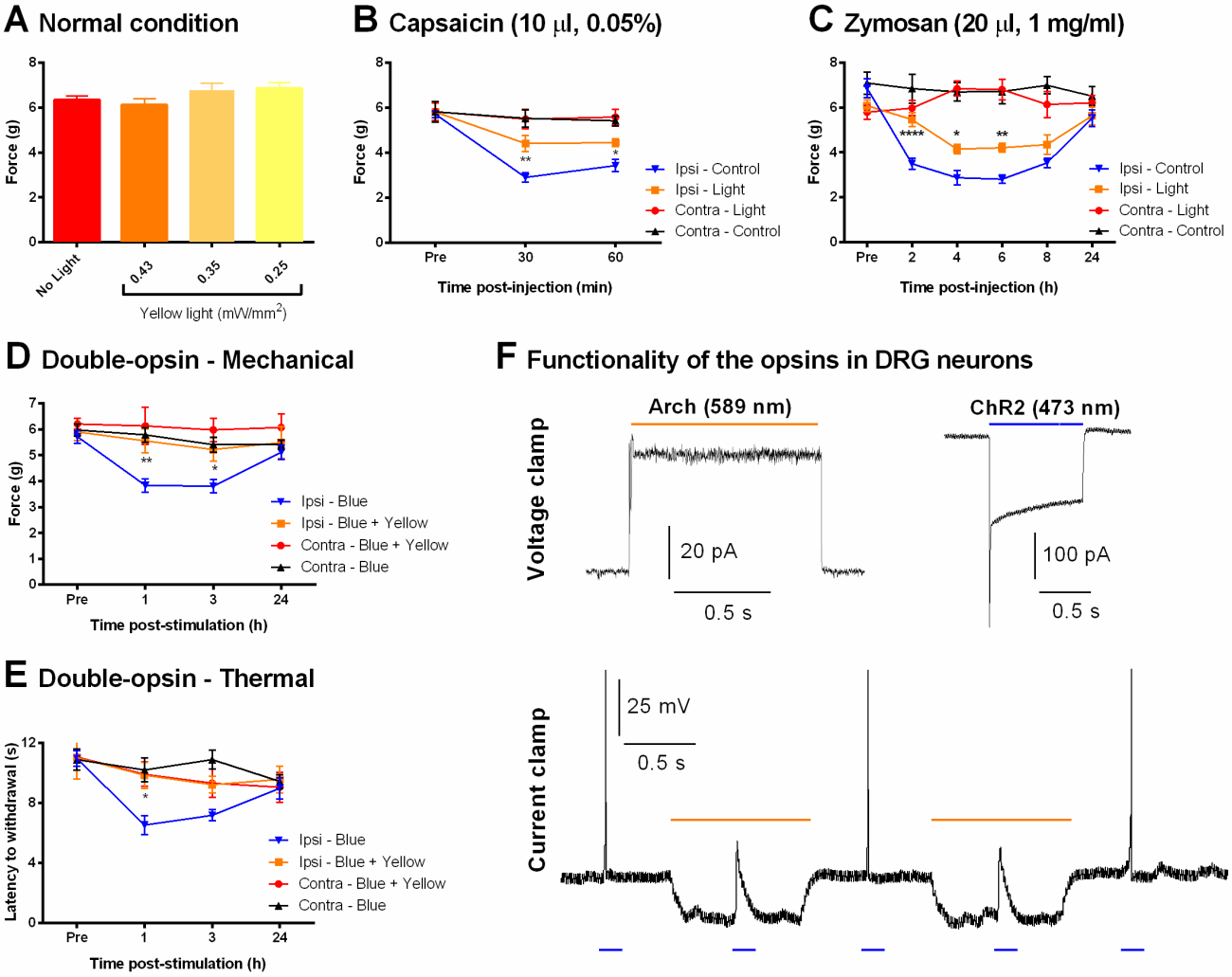

eNeuro Accepted Manuscript

A Mechanical sensitivity - Zymosan (20 μl, 1 mg/ml)

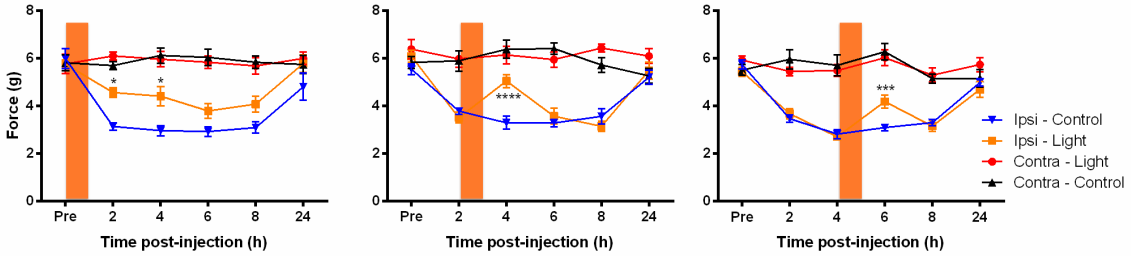

B Thermal sensitivity - CFA (25 μl, 0.5 mg/ml)

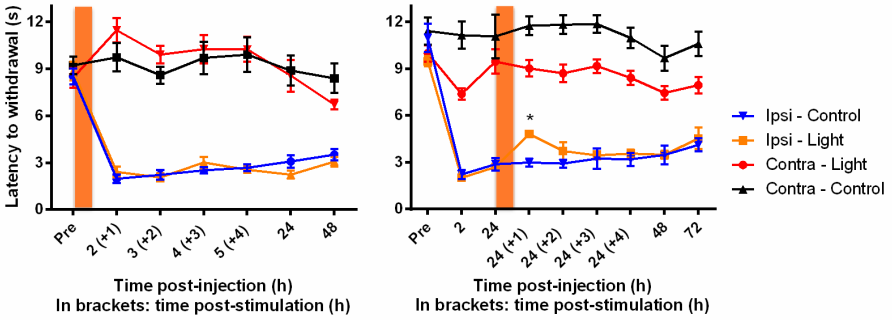

C Thermal sensitivity - naïve

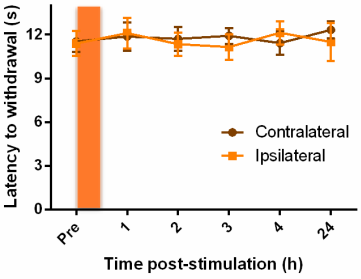

D Arch functionality under repetitive 3 s ON, 1 s OFF stimulations

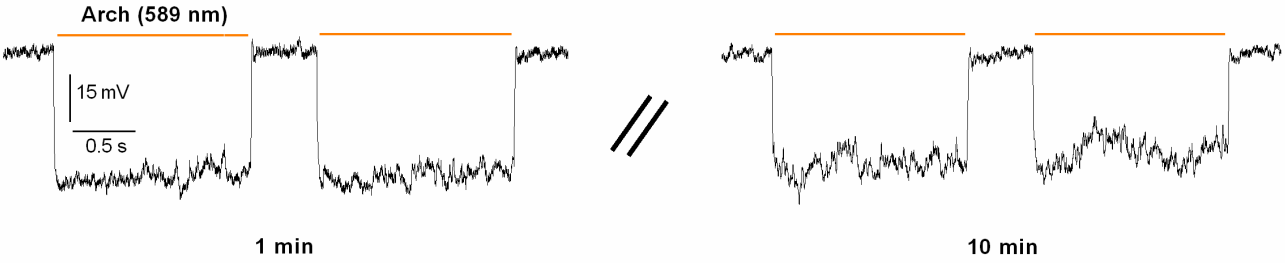

eNeuro Accepted Manuscript
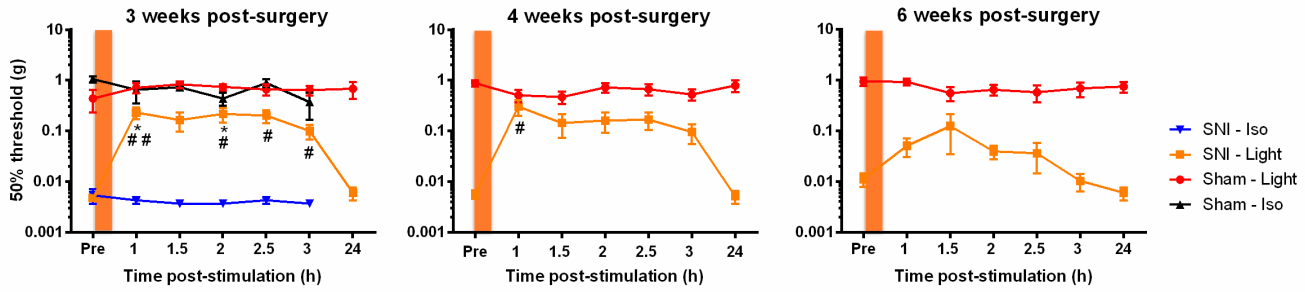
Mechanical sensitivity - SNI